High-fidelity contact pseudopotentials and p-wave superconductivity

P.O. Bugnion, R.J. Needs, and G.J. Conduit

Cavendish Laboratory, J.J. Thomson Avenue, Cambridge, CB3 0HE, United Kingdom

(Dated: March 4, 2014)

We develop ultratransferable pseudopotentials for the contact interaction that are 100 times more accurate than contemporary approximations. The pseudopotential offers scattering properties very similar to the contact potential, has a smooth profile to accelerate numerics by a factor of up to 4,000, and, for positive scattering lengths, does not support an unwanted bound state. We demonstrate these advantages in a Diffusion Monte Carlo study of fermions with repulsive interactions, delivering the first numerical evidence for the formation of a p-wave superconducting state.

Interparticle interactions are central to our understanding of correlated phenomena, but the ubiquitous Coulomb and contact interparticle potentials diverge on coalescence, impeding leading numerical methods. The contact interparticle potential is realized in both ultracold atomic gases and idealized screened electrons, making it an ideal testbed for developing ultratransferable pseudopotentials. Common approximations to the contact interaction display incorrect variations in the scattering phase shift with incident particle energy and can harbor undesired bound states [1–9]. We develop a formalism for generating a bespoke pseudopotential for the contact interaction that offers accurate scattering properties and has no superfluous bound states. These advantages allow us to deliver the first numerical evidence for a p-wave superconducting instability in a fermionic gas with repulsive interactions.

The contact interaction is characterized by a scattering length a that parameterizes the variation of the scattering phase shift with incident energy. The contact interaction comes in three flavors: sufficiently deep to trap a two-body bound state ($a > 0$), weakly attractive with no bound state ($a < 0$), and repulsive ($a > 0$). Contemporary numerical simulations of both the bound state and weak attractive interactions adopt a finite ranged square well or Pöschl-Teller interaction. These simulations have delivered crucial insights into the BEC-BCS crossover [3, 10], Bose gases [4], and few atom physics [5–7]. However, the finite range imbues the potential with incorrect scattering properties. While reducing the range of the potential alleviates this, it slows numerical calculations. The third category of contact potentials gives repulsive interactions that drive itinerant ferromagnetism in Fermi gases [1, 2, 8], a Tonks-Girardeau gas [4], and a Bose gas [9]. The repulsive interaction is the first excited state of the bound state potential so both have $a > 0$, but in ultracold atomic gas experiments [11] the upper branch is protected by a slow three-body loss process. To simulate repulsive interactions the first option is to adopt a finite-ranged attractive potential [1, 2]. However, to avoid forming the bound state, the trial wave function is restricted to the Hartree-Fock excited state solution with no variational parameters, leading to a poor estimate of the energy. Alternatively, one can adopt a repulsive top-hat potential [8] potential with no bound state. However, this has a finite range greater than the scattering length, resulting in an incorrect scattering phase shift. The difficulty of simulating repulsive interactions means that there are important open questions about fermionic gases: is the ground state of a strongly interacting fermionic system ferromagnetic [8, 12–18]; is the ferromagnetic transition first or second order; and whether exotic phases that emerge around quantum criticality include a spin spiral [8], nematic phase [15, 19, 20], and a counterintuitive p-wave superconductor [21]. The p-wave superconductor was suggested by perturbation theory [22–27] and has been observed in experiment [28–34], but has never been seen by numerics.

We develop a general ultratransferable pseudopotential for the contact interaction. We test its accuracy using the exactly soluble system of two trapped atoms, verify the first order itinerant ferromagnet transition, and finally present the first numerical evidence for a p-wave superconducting instability.

DERIVATION OF THE PSEUDOPOTENTIAL

To construct the pseudopotential we study the two-body problem: two fermions in their center-of-mass frame with wavevector $k \geq 0$ and angular momentum quantum number ℓ. The Hamiltonian in atomic units ($\hbar = m = 1$) is $-\frac{\nabla^2}{2}\psi + V(r)\psi = \frac{k^2}{2}\psi$, with the contact potential $V(r) = 2\pi a \delta(r)\frac{\partial}{\partial r}r$ [35]. The scattering states are $\psi_{k,\ell}^{\text{cont}} = \sin[kr - \delta_\ell^{\text{cont}}]/kr$, where δ_ℓ is the scattering phase shift in angular momentum channel ℓ. We seek a pseudopotential that (i) reproduces the correct phase shifts over the range of wavevectors $0 < k \lesssim 2k_{\text{F}}$, where k_{F} is the Fermi wavevector, (ii) supports no superfluous bound states to be compatible with ground state methods and (iii) is smooth and broad to accelerate numerical calculations. We first focus on positive scattering lengths $a > 0$, with no bound state. We describe four families of pseudopotentials: hard sphere, soft sphere (top hat), the
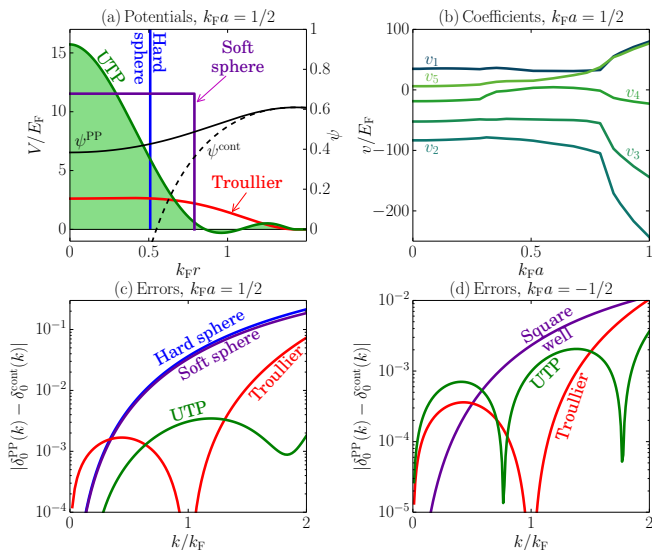
FIG. 1. (Color online) (a) The pseudopotentials at $k_{\rm F}a = 1/2$ on the repulsive branch. UTP denotes the ultratransferable pseudopotential. (b) The first five coefficients for the ultratransferable potential at $k_{\rm F}a = 1/2$. (c) The errors in phase shifts for the repulsive branch at $k_{\rm F}a = 1/2$. (d) The errors in phase shifts for the attractive branch at $k_{\rm F}a = -1/2$.

Troullier-Martins form of norm-conserving pseudopotentials [36, 37] and the new ultratransferable pseudopotential.

The usual approach [1, 8] starts from the low energy expansion for the s-wave scattering phase shift $\cot\delta_0 = -\frac{1}{ka} + \frac{1}{2}kr_{\rm eff} + \mathcal{O}(k^3)$ where $r_{\rm eff}$ is the "effective range" of the potential. For a contact potential, $r_{\rm eff}$ and all higher order terms are zero. Perhaps the simplest pseudopotential is a hard sphere potential with radius a. This reproduces the correct scattering length a, thus delivering the correct phase shift for $k = 0$. However, the hard sphere has an effective range $r_{\rm eff} = 2a/3$. Fig. 1(c) shows that this causes significant deviations in scattering power for $k > 0$.

To improve the scattering phase shift, Ref. [8] adopted a soft sphere potential: $V(r) = V_0\Theta(r - R)$, with V_0 and R chosen to reproduce the correct scattering length $a = R(1 - \tanh\gamma/\gamma)$ and effective range $r_{\rm eff} = R[1 + \frac{3\tanh\gamma - \gamma(3+\gamma^2)}{3\gamma(\gamma-\tanh\gamma)^2}] = 0$, where $\gamma = R\sqrt{2V_0}$. The first two terms in the low energy expansion of the phase shift are now correct, leading to a small reduction in phase shift error in Fig. 1(c).

The two potentials considered so far display incorrect behavior for larger wavevectors due to the focus on reproducing the correct $k = 0$ scattering behavior. To improve the accuracy we turn to the Troullier-Martins [36] formalism developed for constructing attractive electron-ion pseudopotentials. These pseudopotentials reproduce both the correct phase shift and its derivative with respect to energy at a prescribed calibration energy (when

constructing an electron-ion pseudopotential, this is the bound state energy in an isolated atom [37–42]). By calibrating at the energy corresponding to the median incident scattering wavevector $k = k_{\rm F}$, we reduce the errors in the scattering phase shift over a broad range of wavevectors. This delivers the pseudopotential shown in Fig. 1(a) that is smooth, leading to improved numerical stability and efficiency. Fig. 1(c) demonstrates that this potential is exact at the calibration wavevector $k = k_{\rm F}$ and delivers a marked decrease in phase shift error across all wavevectors.

The three potentials deliver a significant progression in accuracy. The hard sphere potential reproduces the correct scattering behavior at $k = 0$. Both the soft sphere and Troullier-Martins potential are transferable: the former producing correct scattering around $k = 0$ and the latter around $k \sim k_{\rm F}$ The significant improvement delivered by the Troullier-Martins potential encourages us to develop the formalism to propose an *ultratransferable* pseudopotential that produces accurate phase shifts over all of the wavevectors occupied in a Fermi gas.

To develop ultransferable pseudopotentials we continue to focus on the contact potential, though the methodology can be readily generalized to other interparticle interactions. We construct a pseudopotential that is identical to the contact potential outside of a cutoff radius r_c, but inside has a continuous first derivative at both $r = 0$ and $r = r_c$,

$$\frac{V(r)}{E_{\rm F}} = \begin{cases} \left(1 - \frac{r}{r_c}\right)^2 \left[v_1\left(\frac{1}{2} + \frac{r}{r_c}\right) + \sum_{i=2}^{N_{\rm v}} v_i\left(\frac{r}{r_c}\right)^i\right] & r \le r_c \\ 0 & r > r_c, \end{cases}$$

with $N_{\rm v} = 9$. We choose the cutoff radius to correspond to the first anti-node of the true wavefunction By choosing a cutoff that is beyond the first node in the wavefunction, we guarantee that the pseudopotential will not harbor a bound state, as demonstrated in Fig. 1(a). We calculate the scattering solution $\psi_{k,\ell}^{\rm PP}(r)$ of the pseudopotential numerically to determine the phase shift $\delta_\ell^{\rm PP}(k(k))$. The difference in the scattering phase shift δ_ℓ of the potentials is characterized by the mean squared error in the phase shifts at the cutoff radius,

$$\langle(\delta_\ell^{\rm PP} - \delta_\ell^{\rm cont})^2\rangle = \int_0^{2k_{\rm F}} \left[\delta_\ell^{\rm PP}(k) - \delta_\ell^{\rm cont}(k)\right]^2 {\rm d}k,$$

that is integrated over all wavevectors $0 \le k \le 2k_{\rm F}$ of interest. The integrand can be convolved with a density of states to emphasize k values of interest. We seek the variational parameters $\{v_i\}$ that minimize the deviation $\langle(\delta_\ell^{\rm PP} - \delta_\ell^{\rm cont})^2\rangle$ to determine the pseudopotential that delivers the best approximation for the contact potential. As demonstrated in Fig. 1(c), this potential delivers an error in δ_0 of less than 10^{-3} for all wavevectors $0 \le k \le 2k_{\rm F}$ found in a Fermi gas, corresponding to an

improvement of two orders of magnitude over previously used pseudopotentials.

The pseudopotentials constructed will have finite scattering amplitude in the p-wave and higher angular momentum channels. The contact potential, by contrast, scatters only in the s-wave channel $|s\rangle$. This can be solved by using a non-local pseudopotential [43, 44] $\hat{V} = |s\rangle V(r)\langle s|$, where $\langle \mathbf{r}|s\rangle = Y_0^0(\mathbf{r})$, with the spherical harmonic Y_0^0 centered on either of the interacting particles. This potential only acts on the s-wave component of the relative wavefunction. Additional accuracy could also be gained by using different projectors for different energy ranges [45, 46].

Attractive branch: We can use a similar procedure to derive pseudopotentials for the attractive branch $a < 0$. For the attractive case, the cutoff can be arbitrarily reduced to generate a potential that tends to the contact limit, at the cost of computational efficiency. For example, in Monte Carlo simulations, the sampling efficiency is approximately proportional to r_c^3. In Fig. 1 we adopt a cutoff $r_c = 1/2k_F$, and compare to the square well potential with cutoff $r_c = 0.01\sqrt[3]{3\pi^2}/k_F$ in Ref. [3]. Both the Troullier-Martins pseudopotential and the ultratransferable pseudopotential have an average error approximately 10 times smaller than the square well potential, but their larger cutoff allows them to be sampled 4,000 times more efficiently.

Bound state: To construct a pseudopotential for the bound state (corresponding to $a > 0$), we follow the Troullier-Martins prescription [36]. We calibrate the pseudopotential at the binding energy $E = -1/2a^2$. The cutoff is constructed in the same manner as for the attractive branch, delivering a similar improvement in efficiency.

ATOMS IN A TRAP

We have developed a pseudopotential that delivers the correct scattering phase shift for an isolated system. To test the pseudopotential we turn to an experimentally realizable configuration [47, 48]: two atoms in a spherical harmonic trap with frequency ω and characteristic length $d = 1/\sqrt{\omega}$. For all three types of interaction shown in Fig. 2(d) this system has an analytical solution [35] that we can benchmark against, forming an ideal test in an inhomogeneous environment. Moreover, the exact solution extends to excited states, allowing us to test the performance of the pseudopotential across a wide range of energy levels to provide a firm foundation from which to study the many-body system.

Ground state: We first compare the pseudopotential estimates of the ground state energy to the exact analytical solution [35]. For the repulsive and attractive branches the hard/soft sphere potentials deliver $\sim 1\%$ error in the energy, whilst both the Troullier-Martins and
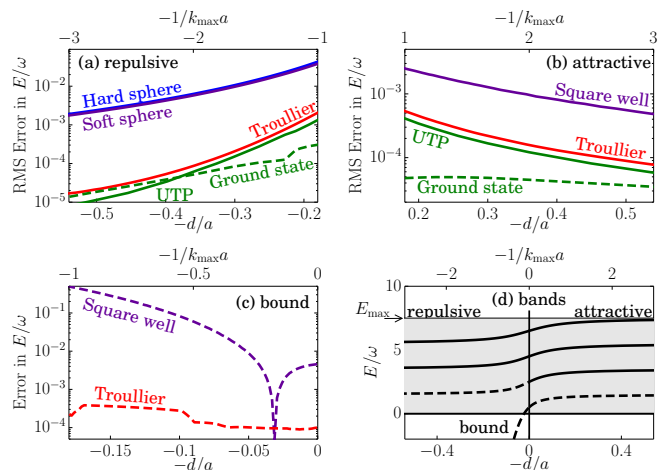

FIG. 2. (Color online) Mean squared error in total energy for two atoms in a harmonic trap, for all bands below $E_{\max}$ (solid lines). (a) The error for repulsive interactions ($k_F a > 0$). UTP denotes the ultratransferable pseudopotential. The dashed line denotes the error in the ground state energy with the ultratransferable pseudopotential. (b) The pseudopotential error for attractive interactions ($k_F a < 0$). (c) The pseudopotential error in the bound state energy. (d) The band diagram for two atoms in a harmonic trap, calculated following Ref. [35].

ultratransferable pseudopotentials (shown in Fig. 2(a,b)) are significantly more accurate with a $\sim 0.01\%$ error. Finally we examine the bound state energy in Fig. 2(c). Both the square well and Troullier-Martins formalism give the exact ground state energy for two atoms in isolation. However, the trapping potential introduces inhomogeneity, so the square well potential gives a $\sim 10\%$ error in the ground state energy, whereas the Troullier-Martins pseudopotential gives a $\sim 0.01\%$ error. This affirms the benefits of using a pseudopotential that is robust against changes in the local environment. The success of the Troullier-Martins and ultratransferable formalism at describing the ground state is all the more significant considering these pseudopotentials aim to describe the correct scattering properties over a range of energies. We would therefore expect them to perform even better when modeling the excited states of the trap.

Excited states: We now turn to examine the predictions for the excited states in the repulsive and attractive branches. Due to the shell structure, the excited states of a few-body system are related to the ground state of a many-body system [7], allowing us to probe the performance expected from the pseudopotential in a many-body setting. We consider states up to a maximum energy $E_{\max} = 7.5\hbar\omega$, corresponding to 112 non-interacting atoms in the trap. In Fig. 2(a,b) the Troullier-Martins pseudopotential has a mean squared error averaged over all bands below $E_{\max}$ that is between 10 and 100 times lower than existing pseudopotentials. The ultratransfer-
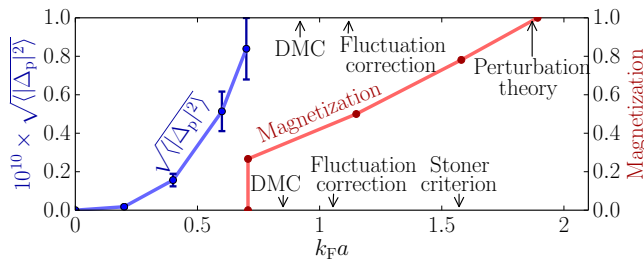
FIG. 3. (Color online) The magnetic phase diagram and emergence of p-wave superconducting order. The error bars on the magnetization line are smaller than the markers. Labels show the predicted interaction strength for the onset of magnetization and entry into the fully polarized state from previous works [1, 8, 12, 17, 56, 57].

able pseudopotential is a further factor of 2 more accurate. Additionally, when modeling the attractive branch, the Troullier-Martins and the ultratransferable formalism are 4,000 times more efficient, due to their larger cutoffs.

REPULSIVE FERMIONS

Having verified that the pseudopotentials reproduce the correct scattering phase shift and bound state energy for two harmonically trapped atoms, we now exploit their accuracy to study two unsolved questions in many-body ferromagnetic metals tuned near quantum criticality: the nature of the ferromagnetic phase transition and presence of p-wave superconducting correlations.

Quantum Monte Carlo: We use fixed-node Diffusion Monte Carlo (DMC) [49] implemented in the CASINO code [50], with a trial wavefunction $\Psi = e^J D_\uparrow D_\downarrow$, where D_α denotes a Slater determinant of N_α plane waves. The Jastrow factor is taken to be

$$J = \sum_{\substack{j \neq i \\ \alpha, \beta \in \{\uparrow, \downarrow\}}} \left(1 - \frac{|\mathbf{r}_i - \mathbf{r}_j|}{L^u_{\alpha\beta}}\right)^2 u_{\alpha\beta}(|\mathbf{r}_i - \mathbf{r}_j|)\Theta(L^u_{\alpha\beta} - |\mathbf{r}_i - \mathbf{r}_j|),$$

where $u_{\alpha\beta}$ is a polynomial whose parameters we optimize in a Variational Monte Carlo (VMC) calculation and $L^u_{\alpha\beta}$ is a cutoff length [51]. We model spin polarized systems by performing calculations for $N_\uparrow = 81$ and $N_\downarrow \in \{81, 57, 33, 27, 19, 7, 1\}$ that correspond to filled shells. This guarantees that the trial wavefunction is an eigenstate of the total spin operator $\hat{S}^2$ and the spatial symmetry operators of the cubic lattice.

We use a backflow transformation [2, 52] in the construction of the orbitals that enter the Slater determinant, with the replacement $\mathbf{r}_{i\sigma} \to \mathbf{r}_{i\sigma} + \sum_{\alpha,\beta \in \{\uparrow,\downarrow\}}^{j \neq i}(\mathbf{r}_i - \mathbf{r}_j)\eta_{ij}^{\alpha\beta}(|\mathbf{r}_i - \mathbf{r}_j|)$ where $\eta_{ij}^{\alpha\beta}(r) = (1 - r/L^\eta_{\alpha\beta})^2\Theta(L^\eta_{\alpha\beta} - r)p_{\alpha\beta}(r)$, $p_{\alpha\beta}$ is a polynomial whose parameters are optimized in VMC, and $L^\eta_{\alpha\beta}$ is a cutoff length. We reduce

finite size effects by twist averaging [53–55] and correct the non-interacting kinetic energy of the finite sized system with that of the corresponding infinite system [1].

Ferromagnetic phase transition: In Fig. 3 we observe a first order phase transition to a partially polarized state at $k_{\mathrm{F}}a = 0.71$, markedly lower than previous DMC predictions of $k_{\mathrm{F}}a \sim 0.85$ [1, 8]. The system becomes fully polarized at $k_{\mathrm{F}}a = 1.89$, close to the theoretical prediction of 1.87 [56, 57]. This is significantly larger than the values calculated previously using DMC [1, 8], demonstrating the quantitative benefits of using a high fidelity pseudopotential. The presence of the first order transition is consistent with theory [8, 14, 16, 17] and with the ferromagnetic transition seen in experiments on heavy fermion materials [58].

P-wave superconductivity can be understood by considering two up-spin electrons in a fermionic gas with repulsive interactions, each surrounded by a fluctuating magnetic polarization cloud. As the electrons coalesce the magnetic fluctuations (that drove the first order ferromagnetic transition) reinforce to create an effective attractive interaction, inducing p-wave superconducting order [34, 59]. The p-wave superconducting state has been observed in experiments on ferromagnetic superconductors [28–34], and has been modeled by a contact interaction in perturbation theory [22–27], but has never been observed in numerics. Equipped with a pseudopotential that reproduces the contact interaction with high fidelity and whose broad profile leads to improved efficiency, we search for p-wave superconducting order.

The p-wave superconducting order is defined by the order parameter $\Delta_{\mathbf{k}} = \sum_{\mathbf{k}'} V_{\mathbf{k}\mathbf{k}'}\langle c_{\mathbf{k}\uparrow}c_{-\mathbf{k}\uparrow}\rangle$. This must be recast into an operator in the position representation and projected onto the p-wave channel. Effecting this transformation results in the projection of the off-diagonal long-range order in the two-body reduced density matrix onto the p-wave channel [10, 60, 61]

$$\langle|\Delta_{\mathrm{p}}|^2\rangle = -\frac{(4\pi k_{\mathrm{F}}a)^2}{81\Omega^2}\lim_{\substack{\mathbf{R} \\ \to \infty}}\iint \mathbf{r}\cdot\mathbf{r}'\langle c^\dagger_{\frac{\mathbf{r}}{2}}c^\dagger_{-\frac{\mathbf{r}}{2}}c_{\mathbf{R}+\frac{\mathbf{r}'}{2}}c_{\mathbf{R}-\frac{\mathbf{r}'}{2}}\rangle\mathrm{d}\mathbf{r}\mathrm{d}\mathbf{r}',$$

where Ω is the simulation cell volume. The expectation value is zero for the Slater determinant trial wavefunction $D_\uparrow D_\downarrow$ with no electron-electron correlations. However, if we insert the full trial wavefunction $\psi = e^J D_\uparrow D_\downarrow$ into the expectation value and expand in the limit of small electron separation, we find that $\langle|\Delta_{\mathrm{p}}|^2\rangle \approx 2^{10}3^{-15}5^{-2}7^{-1}(k_{\mathrm{F}}c)^8 u_{\uparrow\uparrow}(0)$, connecting the superconducting correlations to the up-spin correlation term in the Jastrow factor. This verifies that the trial wave function has the variational freedom to exhibit a superconducting instability.

In Fig. 3 we show the emergence of the p-wave superconducting order parameter with increasing interaction strength. The p-wave superconductor may be enhanced in the partially polarized phase [27], but is destroyed in

the fully polarized state as there can be no magnetic fluctuations. The delicacy of the superconducting order requires a high-fidelity pseudopotential. The emergence of the p-wave superconducting order provides the first verification of the magnetic fluctuations theory valid at high interaction strengths, confirming the NMR measurements on UCoGe [34].

DISCUSSION

We have developed a high fidelity pseudopotential for the contact interaction. The pseudopotential is ultratranserable, delivering accurate scattering properties over all wavevectors $0 \leq k \leq 2k_\mathrm{F}$ in a Fermi gas and its smoothness accelerates computation. This pseudopotential allowed us to characterize the first order itinerant ferromagnetic transition and present the first computational evidence for a p-wave superconducting state.

The performance and portability of the pseudopotential makes it widely applicable across first principles methods including VMC, DMC, coupled cluster theory, and configuration interaction. The formalism developed can also be applied more widely in scattering problems in condensed matter to develop pseudopotentials, including the repulsive Coulomb interaction and dipolar interactions.

[1] S. Pilati, G. Bertaina, S. Giorgini, and M. Troyer, Phys. Rev. Lett. **105**, 030405 (2010).
[2] S.-Y. Chang, M. Randeria, and N. Trivedi, PNAS **108**, 51 (2010).
[3] G.E. Astrakharchik, J. Boronat, J. Casulleras, and S. Giorgini, Phys. Rev. Lett. **93**, 200404 (2004).
[4] G.E. Astrakharchik, D. Blume, S. Giorgini, and B.E. Granger, Phys. Rev. Lett. **92**, 030402 (2004).
[5] P.O. Bugnion and G.J. Conduit, Phys. Rev. A **87**, 060502(R) (2013).
[6] P.O. Bugnion and G.J. Conduit, Phys. Rev. A **88**, 013601 (2013).
[7] P.O. Bugnion, J.A. Lofthouse, and G.J. Conduit, Phys. Rev. Lett. **111**, 045301 (2013).
[8] G.J. Conduit, A.G. Green, and B.D. Simons, Phys. Rev. Lett. **103**, 207201 (2009).
[9] S. Giorgini, J. Boronat, and J. Casulleras, Phys. Rev. A **60**, 5129 (1999).
[10] A.J. Morris, P. López Ríos and R.J. Needs, Phys. Rev. A **81**, 033619 (2010).
[11] G.-B. Jo *et al.*, Science **325**, 1521 (2009).
[12] G.J. Conduit and B.D. Simons, Phys. Rev. A **79**, 053606 (2009).
[13] H. Zhai, Phys. Rev. A **80**, 051605(R) (2009).
[14] D.L. Maslov and A.V. Chubukov, Phys. Rev. B **79**, 075112 (2009).
[15] A.V. Chubukov and D.L. Maslov, Phys. Rev. Lett. **103**, 216401 (2009).
[16] C.J. Pedder, F. Krüger, and A.G. Green, Phys. Rev. B **88**, 165109 (2013).
[17] R.A. Duine and A.H. MacDonald, Phys. Rev. Lett. **95**, 230403 (2005).
[18] G.J. Conduit and B.D. Simons, Phys. Rev. Lett. **103**, 200403 (2009).
[19] D.L. Maslov and A.V. Chubukov, Phys. Rev. B **81**, 045110 (2010).
[20] U. Karahasanovic, F. Krüger, and A.G. Green, Phys. Rev. B **85**, 165111 (2012).
[21] R. Balian and N.R. Werthamer, Phys. Rev. **131**, 1553 (1963).
[22] D. Fay and J. Appel, Phys. Rev. B **22**, 3173 (1980).
[23] N.D. Mathur *et al.*, Nature **394**, 39 (1998).
[24] R. Roussev and A. J. Millis, Phys. Rev. B **63**, 140504(R) (2001).
[25] T.R. Kirkpatrick, D. Belitz, T. Vojta, and R. Narayanan, Phys. Rev. Lett **87**, 127003 (2001).
[26] Z. Wang, W. Mao, and K. Bedell, Phys. Rev. Lett. **87**, 257001 (2001).
[27] G.J. Conduit, C.J. Pedder, and A.G. Green, Phys. Rev. B **87**, 121112(R) (2013).
[28] S. Watanabe and K. Miyake, J. Phys. Chem. Solids **63**, 1465 (2002).
[29] S.S. Saxena, P. Agarwal, K. Ahilan, F.M. Grosche, R.K.W. Haselwimmer, M.J. Steiner, E. Pugh, I.R. Walker, S.R. Julian, P. Monthoux, G.G. Lonzarich, A. Huxley, I. Sheikin, D. Braithwaite, and J. Flouquet, Nature (London) **406**, 587 (2000).
[30] A. Huxley *et al.*, Phys. Rev. B **63**, 144519 (2001).
[31] D. Aoki, A. Huxley, E. Ressouche, D. Braithwaite, J. Flouquet, J.-P. Brison, E. Lhotel, and C. Paulsen, Nature (London) **413**, 613 (2001).
[32] N.T. Huy, A. Gasparini, D.E. de Nijs, Y. Huang, J.C.P. Klaasse, T. Gortenmulder, A. de Visser, A. Hamann, T. Görlach, and H.V. Löhneysen, Phys. Rev. Lett. **99**, 067006 (2007).
[33] A. Gasparini, Y. K. Huang, N. T. Huy, J. C. P. Klasse, T. Naka, E. Slooten, and A. De Visser, J. Low Temp. Phys. **161**, 134 (2010).
[34] T. Hattori, Y. Ihara, Y. Nakai, K. Ishida, Y. Tada, S. Fujimoto, N. Kawakami, E. Osaki, K. Deguchi, N.K. Sato, and I. Satoh, Phys. Rev. Lett. **108**, 066403 (2012).
[35] T. Busch, B.G. Englert, K. Rzazewski, and M. Wilkens, Foundations of Physics **28**, 549 (1998).
[36] N. Troullier and J.L. Martins, Phys. Rev. B **43**, 1993 (1991).
[37] D.R. Hamann, M. Schlüter, and C. Chiang, Phys. Rev. Lett. **43**, 1494 (1979).
[38] A. Zunger and M.L. Cohen, Phys. Rev. B **20**, 4082 (1979).
[39] G.B. Bachelet, D.R. Hamann, and M. Schlüter, Phys. Rev. B **26**, 4199 (1982).
[40] D.R. Hamann, Phys. Rev. B, **40**, 2980 (1989).
[41] A.M. Rappe, K.M. Rabe, E. Kaxiras, and J.D. Joannopoulos, Phys. Rev. B **41**, 1227 (1990).
[42] J.S. Lin, A. Qteish, M.C. Payne and V. Heine, Phys. Rev. B **47**, 4174 (1993).
[43] L. Kleinman and D.M. Bylander, Phys. Rev. Lett. **48**, 1425 (1982).

[44] S. Fahy, X.W. Wang and S.G. Louie, Phys. Rev. B **42** 3503 (1990).

[45] D. Vanderbilt, Phys. Rev. B **41**, 7892 (1990).

[46] P.E. Blöchl, Phys. Rev. B **50**, 17953 (1994).

[47] F. Serwane, G. Zürn, T. Lompe, T.B. Ottenstein, A.N. Wenz, and S. Jochim, Science **332**, 336 (2011).

[48] G. Zürn, F. Serwane, T. Lompe, A.N. Wenz, M.G. Ries, J.E. Bohn, and S. Jochim, Phys. Rev. Lett **108**, 075303 (2012).

[49] C.J. Umrigar, M.P. Nightingale, and K.J. Runge, J. Chem. Phys. **99**, 2865 (1993).

[50] R.J. Needs, M.D. Towler, N.D. Drummond, and P. López Ríos, J. Phys.: Condensed Matter **22**, 023201 (2010).

[51] N.D. Drummond, M.D. Towler, and R.J. Needs, Phys. Rev. B **70**, 235119 (2004).

[52] P. López Ríos, A. Ma, N.D. Drummond, M.D. Towler, and R.J. Needs, Phys. Rev. E **74**, 066701 (2006).

[53] C. Lin, F.H. Zong, and D.M. Ceperley, Phys. Rev. E **64**, 016702 (2001).

[54] G. Rajagopal, R.J. Needs, S.D. Kenny, W.M.C. Foulkes, and A. James, Phys. Rev. Lett. **73**, 1959 (1994).

[55] G. Rajagopal, R.J. Needs, A. James, S.D. Kenny, and W.M.C. Foulkes, Phys. Rev. B. **51**, 10591 (1995).

[56] P. Massignan and G.M. Bruun, Eur. Phys. J. D **65**, 83 (2011).

[57] X. Cui and H. Zhai, Phys. Rev. A **81**, 041602(R) (2010).

[58] D. Belitz and T.R. Kirkpatrick, arXiv:1204.0873.

[59] S.R. Julian, Physics **5**, 17 (2012).

[60] L.K. Wagner, J. Chem. Phys. **138**, 094106 (2013).

[61] C.N. Yang, Rev. Mod. Phys. **34**, 694 (1962).